American Mineralogist, Volume 85, pages 593–599, 2000

Crystal chemistry of the new mineral brandholzite, $Mg(H_2O)_6[Sb(OH)_6]_2$, and of the synthetic analogues $M^{2+}(H_2O)_6[Sb(OH)_6]_2$ (M^{2+} = Mg, Co)

ALEXANDRA FRIEDRICH,[1,*] MANFRED WILDNER,[1,†] EKKEHART TILLMANNS,[1] AND PETER L. MERZ[2]

[1]Institut für Mineralogie und Kristallographie, Universität Wien, Geozentrum, Althanstrasse 14, A-1090 Wien, Austria
[2]Institut für Mineralogie und Kristallstrukturlehre, Universität Würzburg, Am Hubland, D-97074 Würzburg, Germany

ABSTRACT

Brandholzite, a new magnesium antimony hydroxide hydrate mineral, $Mg(H_2O)_6[Sb(OH)_6]_2$, has been discovered in Au-Sb-Quartz veins of the former mining district of Brandholz-Goldkronach, Fichtelgebirge, Germany. The new mineral is associated with stibnite and antimony-ochers and forms colorless, platelike crystals up to ~1 mm in size. Natural as well as synthetic samples obtained by slow evaporation of an aqueous solution exhibit $\{10\bar{1}0\}$ twinning, leading to a pronounced $\bar{3}1m$ pseudo-symmetry. The crystal structures of brandholzite and its synthetic analogue were investigated using single crystal X-ray CCD data: trigonal, space group $P3$, $Z = 6$, $a = 16.119(1)$ Å, $c = 9.868(1)$ Å, $R1 = 0.034$ for 14788 $F_o > 4\sigma(F_o)$ (brandholzite), and $a = 16.113(1)$ Å, $c = 9.868(1)$ Å, $R1 = 0.029$ for 16624 $F_o > 4\sigma(F_o)$ (synthetic analogue) and 525 variable parameters each. The structures are isotypic with bottinoite, $Ni(H_2O)_6[Sb(OH)_6]_2$, and are built up by nearly regularly shaped, isolated $Mg(H_2O)_6$ and $Sb(OH)_6$ octahedra which are interconnected by hydrogen bonds only. The strongest lines in the powder pattern are [*d*-value (Å), *I*, *hkl*]: 4.636, 100, (300); 3.392, 70, (302); 4.946, 50, (002); 2.356, 40, (332). At 589 nm, the mineral is optically uniaxial negative with refractive indices $n_\omega = 1.570(2)$ and $n_\varepsilon = 1.569(2)$. The crystal structure of the pseudo-isotypic synthetic compound $Co(H_2O)_6[Sb(OH)_6]_2$ was also investigated: trigonal, space group $P3$, $a = 16.105(1)$, $c = 9.851(1)$, Z = 6, R1 = 0.051 for 13516 reflections with $F_o > 4\sigma(F_o)$ and 525 parameters. Compared to the Mg-antimonates and bottinoite, a significant rotation of some $Sb(OH)_6$ octahedra is observed in $Co(H_2O)_6[Sb(OH)_6]_2$.

INTRODUCTION

Colorless crystals of an hitherto unknown mineral embedded in a stibnite matrix were found in the Brandholz-Goldkronach area, Fichtelgebirge, Germany, by S. Meier who provided samples to us. Using chemical and thermogravimetric analyses, IR-spectroscopy, and X-ray powder diffractometry, this new mineral was identified as magnesium antimony hydroxide hydrate, $Mg(H_2O)_6[Sb(OH)_6]_2$. An initial structural model for synthetic $Mg(H_2O)_6[Sb(OH)_6]_2$ and isotypic compounds had already been proposed by Beintema (1936). However, the structure determination failed due to the wrong choice of space group ($P\bar{3}1m$) based on the strong $\bar{3}1m$ pseudo-symmetry. Recently, Bonazzi and Mazzi (1996) solved the crystal structure of bottinoite, $Ni(H_2O)_6[Sb(OH)_6]_2$, in space group $P3$ taking $\{10\bar{1}0\}$-twinning into account. Our present single crystal X-ray investigations on brandholzite and synthetic Mg- and $Co(H_2O)_6[Sb(OH)_6]_2$ showed isotypism (respectively pseudo-isotypism for the Co-compound) with bottinoite as well as the presence of $\{10\bar{1}0\}$-twinning in all three compounds. Furthermore, the high quality of our X-ray CCD (charge coupled device) data enabled the refinement of all hydrogen positions and the determination of the complex hydrogen bonding system in brandholzite.

The mineral was named after the type locality of Brandholz. The mineral and its name have been approved by the IMA Commision on New Minerals and Mineral Names prior to publication (no. 98-017). Type material is deposited in the collection of the Institut für Mineralogie und Kristallographie, Universität Wien in Vienna, Austria.

OCCURRENCE AND PARAGENESIS

The former Brandholz-Goldkronach mining district is located in the western part of the Fichtelgebirge in Bavaria, Germany, in the region of a series of paleozoic schists injected with hydrothermal gold-quartz veins. The Fichtelgebirge was formed during the variscan orogeny. In the younger variscan interval, granitic plutons intruded resulting in formation of ore-bearing hydrothermal veins (Stettner 1980). In the Brandholz-Goldkronach area these hydrothermal veins are associated mainly with stibnite, pyrite, and arsenopyrite beneath fahlores, bournonite, sphalerite, and galenite.

Brandholzite was found embedded in a stibnite matrix together with antimony-ochers in the pits Schmidten-Schacht and Jakobi-Schacht of the master lode, the Fürstenzeche. It most probably formed as an alteration product of stibnite within a zone of oxidation.

*Present address: Laboratorium für Kristallographie, ETH Zentrum, Sonneggstrasse 5, CH-8092, Zürich, Switzerland.
†E-mail: manfred.wildner@univie.ac.at

EXPERIMENTAL METHODS

Synthesis

The synthesis of $Mg(H_2O)_6[Sb(OH)_6]_2$ was described first by Heffter (1852). Our synthesis experiments followed the procedure reported by Haushofer (1880). Starting materials for the Mg- and Co-compound were aqueous solutions of $K[Sb(OH)_6]$, $MgCl_2$, and $CoSO_4 \cdot 7H_2O$. Upon mixing, an amorphous phase precipitated immediately due to the poor solubility of the desired compounds. Single crystals of $Mg(H_2O)_6[Sb(OH)_6]_2$ of excellent quality up to $1.8 \times 1.7 \times 0.4$ mm^3 were then obtained by slow evaporation at room temperature. In the case of $Co(H_2O)_6[Sb(OH)_6]_2$, only a few flat crystals up to $0.4 \times 0.4 \times 0.06$ mm^3 could be obtained.

Physical properties and chemical composition

Crystals of brandholzite were found up to ~1 mm in diameter (but mostly <0.5 mm), often forming roselike aggregates. They show tabular hexagonal habit with predominant forms $\{10\bar{1}0\}$ and {0001}. Crystals are transparent, colorless with a vitreous luster, and a white streak. No fluorescence is observed. Single crystals are brittle without any preferred cleavage, and show conchoidal fracture. A density of 2.65(5) g/cm^3 was measured by flotation in high-density liquids. The Vickers-hardness (VHN) was determined to be 60 kg/mm^2, which corresponds approximately to a Mohs-hardness of 2–3.

The optical constants of natural and synthetic brandholzite were determined on a spindle stage using the immersion method at variable wavelengths. At 589 nm brandholzite is uniaxial optically negative with refractive indices of $n_w = 1.570(2)$ and $n_e = 1.569(2)$.

Synthetic $Co(H_2O)_6[Sb(OH)_6]_2$ shows similar properties, but only forms thin orange-rose hexagonal platelets. The Vickers-hardness is 65 kg/mm^2. $Co(H_2O)_6[Sb(OH)_6]_2$ is uniaxial optically positive with refractive indices of $n_w = 1.589(2)$ and $n_e = 1.592(2)$ at 589 nm.

The chemical composition was investigated by electron microprobe analyses (EMS in Table 1) using a Cameca SX100 (15 kV, 8 nA, 10 µm electron beam diameter) with metallic Sb, MgO, and metallic Co as standards. Qualitative energy- and wavelength-dispersive analyses only showed the presence of Mg and Sb, and Co and Sb, respectively. No other elements could be detected. Due to instability in vacuum and under exposure to the electron beam, detected contents of MgO, CoO, and Sb_2O_5 are higher than the theoretical ones (Table 1). Nevertheless, the Mg/Sb atomic ratio (0.465 for natural and 0.416 for synthetic crystals) and the Co/Sb atomic ratio (0.457) are close to the expected value of 0.5. Dehydration during electron microprobe analysis is responsible for the low derived water contents which do not agree at all with the results from structural and thermogravimetric analyses. Due to the small amounts of natural brandholzite available so far, a complete chemical characterization was performed only on synthetic material. Sb was determined by means of atom absorption spectroscopy (AAS), Mg by flame emission spectroscopy (FES) from a hydrochloric acid solution, employing the method of addition and extrapolation by linear regression (Table 1).

TABLE 1. Results of chemical analyses (wt%) by EMS, AAS, and FES and ideal composition of brandholzite and synthetic $M(H_2O)_6[Sb(OH)_6]_2$ (M = Mg, Co)

	Brandholzite	M = Mg			M = Co	
	EMS*	EMS	AAS/FES	ideal	EMS	Ideal
MO	8.8(2.0)	7.7(1.0)	6.7	6.9	14.9(0.5)	12.2
Sb_2O_5	76.3(3.0)	73.9(2.0)	55.0	55.8	70.5(1.5)	52.5
Sum	85.1	81.6	61.6	62.7	85.4	64.7

***** Range and average obtained from four analyses.

Thermogravimetric analysis (TGA) of synthetic $Mg(H_2O)_6[Sb(OH)_6]_2$ up to 850 °C revealed a total water content of 39.0 wt%, in close agreement with the theoretical value (37.3 wt%). At a heating rate of 1 K/min the weight decreases rapidly with a maximum at 112 °C. Within the temperature range between 150 and 450 °C minor continuous loss of weight is observed. X-ray powder diffraction measurements show that the resulting product is amorphous up to ~700 °C, when it recrystallizes to $MgSb_2O_6$. Based on the more reliable chemical analyses discussed above (AAS, FES, and TGA), the empirical composition $(MgO)_{0.97}(Sb_2O_5)_{0.99}(H_2O)_{12.56}$ is derived, leading to the idealized crystal chemical formula $Mg(H_2O)_6[Sb(OH)_6]_2$.

The agreement between density, refractive indices, and chemical composition was checked by the Gladstone-Dale relationship using the constants of Mandarino (1976). The chemical refractive energies K_C were calculated from the EMS-analyses, which were corrected for the ideal water content. The compatibility indexes $1\text{-}K_P/K_C$ (Mandarino 1981) are 0.029 for brandholzite, 0.028 for synthetic $Mg(H_2O)_6[Sb(OH)_6]_2$, and 0.037 for $Co(H_2O)_6[Sb(OH)_6]_2$, thus characterizing the internal consistency of data for all three compounds as "excellent".

Infrared spectroscopic analysis of synthetic $Mg(H_2O)_6[Sb(OH)_6]_2$ confirmed the presence of H_2O molecules and OH groups involved in intermediate to weak hydrogen bonding. The powder absorption spectrum is quite similar to those described by Balitcheva and Roi (1971) and Franck (1973).

X-ray diffraction measurements

Due to the small quantity of natural material, a X-ray powder diffraction pattern was recorded on a Debye-Scherrer camera using Cu$K\alpha$ radiation. The observed *d*-spacings and estimated intensities agree well with the calculated ones and confirm the identity of brandholzite with synthetic $Mg(H_2O)_6[Sb(OH)_6]_2$ (PDF 40-335). The strongest peaks in the powder pattern of brandholzite are [*d*-value (Å), *I*, *hkl*]: 4.636, 100, (300); 3.392, 70, (302); 4.946, 50, (002); 2.356, 40, (332).

The crystal structures of natural and synthetic $Mg(H_2O)_6[Sb(OH)_6]_2$ as well as of synthetic $Co(H_2O)_6[Sb(OH)_6]_2$ were investigated using single-crystal X-ray CCD data. Intensity data were collected at room temperature using a Nonius Kappa CCD four-circle diffractometer with graphite monochromatized Mo$K\alpha$ radiation. For each compound a total of 457 CCD-frames in several sets of φ- and ω-scans with 2° rotation per frame and 28 mm crystal to detector distance were measured to collect the complete Ewald spheres up to 70° 2θ as well as additional reflections (~80% completeness) up to 2θ = 80°. The extraction of intensity data, including corrections for Lorentz and polarization effects and a pseudo absorption correction by frame scaling, as well as the refinement of lattice parameters from all measured reflections were performed with DENZO-SMN. As

a consequence of the {10$\bar{1}$0} twinning of all investigated crystals, the intensity data show a strong pseudo-symmetry toward Laue class $\bar{3}$1m, which obviously lead to the misinterpretation in the structure investigations of $M(H_2O)_6[Sb(OH)_6]_2$ compounds by Beintema (1936). Bonazzi and Mazzi (1996) identified the correct space group *P*3 and the twinning law with {10$\bar{1}$0} as the twin plane for bottinoite, $Ni(H_2O)_6[Sb(OH)_6]_2$ (refer to their paper for a thorough discussion of various aspects of this twinning mechanism). Hence, the structure refinements on F^2 with SHELXL97 were started with the non-hydrogen atomic coordinates given by Bonazzi and Mazzi (1996). After the refinement with anisotropic displacement parameters, all 48 hydrogen positions could be located in a difference Fourier map of brandholzite and could also be refined applying soft anti-bumping restraints. To reduce the number of independent parameters, one common isotropic displacement factor was refined for the hydrogen atoms to $U(H)_{iso} = 0.037(1)$ Å^2. Moreover, the hydrogen positions in the structures of the synthetic crystals could only be refined by applying strong O-H bond length restraints. Hence, these hydrogen positions (especially in the Co-compound) are less reliable and are therefore not reported.

The structure refinements finally converged to *R*-values of *R*1 = 0.034, *wR*2 = 0.047 for brandholzite, *R*1 = 0.029, *wR*2 = 0.064 for synthetic $Mg(H_2O)_6[Sb(OH)_6]_2$, and *R* = 0.051, *wR*2 = 0.106 for $Co(H_2O)_6[Sb(OH)_6]_2$. The contributions of the respective smaller twin component in these compounds were refined to about 15, 48, and 33%. The high positive residual electron densities observed for both synthetic compounds are most probably caused by stacking faults and local disorder due to fast crystal growth. Crystal data and details of the intensity measurements and structure refinements are in Table 2. The final atomic coordinates and equivalent isotropic displacement parameters (according to Fischer and Tillmanns 1988) for brandholzite and $Co(H_2O)_6[Sb(OH)_6]_2$ are in Table 3, hydrogen positions for brandholzite are in Table 4. Structure parameters for synthetic $Mg(H_2O)_6[Sb(OH)_6]_2$ as well as anisotropic displacement parameters for all compounds are available from the authors on request.

RESULTS AND DISCUSSION

Crystal structures of brandholzite and synthetic $Mg(H_2O)_6[Sb(OH)_6]_2$

General aspects. The crystal structure of brandholzite, $Mg(H_2O)_6[Sb(OH)_6]_2$, is built up by nearly regularly shaped, isolated $Mg(H_2O)_6$ and $Sb(OH)_6$ octahedra which are interconnected by hydrogen bonds only. These octahedra are arranged in two types of layers which are stacked along the *c* axis. One layer consists of $Sb(OH)_6$ octahedra only (Fig. 1), the other of $Mg(H_2O)_6$ and $Sb(OH)_6$ octahedra with a Mg/Sb-ratio of 2:1 (Fig. 2). The resulting compositions of these layers are $\{[Sb(OH)_6]_9\}^{9-}$ and $\{[Sb(OH)_6]_3[Mg(H_2O)_6]_6\}^{9+}$, respectively. The absence of cleavage parallel to the layers can be explained by the topology of the complex hydrogen bonding system, because not only the layers themselves but also the octahedra within each layer are interconnected by hydrogen bonds only.

The structure can also be described as a distorted hexagonal close-packing of oxygen atoms in an ABA'B' stacking sequence (Bonazzi and Mazzi 1996). One-sixth of the octahedral positions are filled with antimony and magnesium atoms, where planes at $z \approx 0$ and 1/2, occupied to one-third, alternate with unfilled planes at $z \approx 1/4$ and 3/4. At $z \approx 0$, two out of nine octahedral voids are occupied by Mg^{2+} and one by Sb^{5+}. At $z \approx 1/2$, only Sb^{5+} fills those gaps. Compared to an ideal closest packing the occupied octahedra are twisted by a small amount as a consequence of the hydrogen bonding system.

$Sb(OH)_6$ and $Mg(H_2O)_6$ octahedra. The octahedral environments of the metal atoms are nearly regular in shape. The overall mean Sb-O bond length in brandholzite, 1.978 Å, cor-

TABLE 2. Summary of crystal data and details of the intensity measurements and structure refinements of brandholzite and synthetic $M(H_2O)_6[Sb(OH)_6]_2$ (M = Mg, Co)

Compound	brandholzite	M = Mg	M = Co
Molecular weight (g/mol)	580.0	580.0	614.6
Space group	P3 (No. 43)	P3 (No. 43)	P3 (No. 43)
a (Å)	16.119(1)	16.113(1)	16.105(1)
c (Å)	9.868(1)	9.868(1)	9.851(1)
Volume (Å^3)	2220.4(1)	2218.8(1)	2212.6(1)
Z	6	6	6
ρ_{calc} (g/cm^3)	2.603	2.604	2.768
Crystal size (mm^3)	0.10 × 0.16 × 0.16	0.15 × 0.17 × 0.25	0.05 × 0.13 × 0.20
Twinning	{10$\bar{1}$0}	{10$\bar{1}$0}	{10$\bar{1}$0}
Twin component (%)	15	48	33
μ(Mo*K*α) (mm^{-1})	3.78	3.79	4.84
Extinction coefficient	1.3×10^{-3}	0.4×10^{-3}	$< 10^{-5}$
$2\theta_{max/complete}$ (°)	80/70	80/70	80/70
Exposure time (sec/frame)	2 × 100	2 × 60	2 × 100
Number of intensity data	136952	147154	152320
Measured reflections	50764	50190	49418
Unique data set	18070	17961	17895
R_i	0.0484	0.0291	0.0617
Reflections with $F_o > 4\sigma(F_o)$	14788	16624	13516
Variables	525	525	525
*R*1 [for $F_o > 4\sigma(F_o)$]	0.0337	0.0285	0.0509
*R*1 (for all F_o)	0.0503	0.0329	0.0791
*wR*2 (for all F_o^2)	0.0473	0.0639	0.1063
$\Delta\rho_{min/max}$ (e$^-$/Å^3)	–0.95/1.72	–1.72/6.64	–2.35/10.69

Notes: $R1 = \Sigma||F_o| - |F_c||/\Sigma|F_o|$; $wR2 = [\Sigma w(F_o^2 - F_c^2)^2/\Sigma wF_o^4]^{1/2}$; $w = 1 / [\sigma^2(F_o^2) + (0.01,0.04,0.05 \times P)^2 + 0,0.2,0 \times P]$; $P = \{[\max \text{ of } (0 \text{ or } F_o^2)] + 2F_c^2\}/3$.

TABLE 3. Atomic coordinates and equivalent isotropic displacement parameters (Å²) of brandholzite and $Co(H_2O)_6[Sb(OH)_6]_2$

	x/a	*y/b*	*z/c*	U_{eq}	*x/a*	*y/b*	*z/c*	U_{eq}
	Brandholzite layer at z ≈ 0				**$Co(H_2O)_6[Sb(OH)_6]_2$ layer at *z* ≈ 0**			
Sb1	0	0	0.00000(0)	0.0109(1)	0	0	0.00000(0)	0.0107(1)
Sb2	2/3	1/3	–0.08211(3)	0.0107(1)	2/3	1/3	–0.00850(7)	0.0116(1)
Sb3	1/3	2/3	0.00883(4)	0.0104(1)	1/3	2/3	–0.09218(6)	0.0118(1)
Mg1	0.33825(7)	0.00882(7)	–0.03108(17)	0.0142(2)	0.33755(7)	–0.00376(6)	–0.03589(13)	0.0165(2)
Mg2	0.66274(8)	–0.00884(7)	–0.04466(17)	0.0149(2)	0.67454(7)	0.00358(7)	–0.05172(11)	0.0146(2)
O1	0.0335(1)	0.1144(1)	–0.1107(2)	0.0176(4)	0.0295(2)	0.1136(3)	–0.1118(4)	0.0168(7)
O2	0.1132(1)	0.0835(1)	0.1123(2)	0.0186(4)	0.1115(3)	0.0847(3)	0.1127(4)	0.0183(8)
O3	0.5822(1)	0.2204(1)	–0.1939(2)	0.0172(4)	0.7470(3)	0.2999(3)	–0.1210(5)	0.0196(8)
O4	0.6962(1)	0.2494(1)	0.0283(2)	0.0170(4)	0.7795(3)	0.4172(3)	0.1031(4)	0.0175(8)
O5	0.3049(1)	0.5543(1)	0.1205(2)	0.0175(4)	0.3625(3)	0.5827(3)	0.0196(4)	0.0189(8)
O6	0.3635(1)	0.7805(1)	–0.1021(2)	0.0176(4)	0.3045(3)	0.7501(3)	–0.2062(5)	0.0205(9)
O7	0.3147(2)	0.0983(1)	–0.1531(2)	0.0241(4)	0.3059(3)	0.0813(3)	–0.1649(5)	0.0222(9)
O8	0.4311(2)	0.1157(2)	0.0942(2)	0.0277(5)	0.4228(3)	0.1141(3)	0.0816(5)	0.0234(10)
O9	0.4532(1)	0.0333(1)	–0.1505(2)	0.0204(4)	0.4526(3)	0.0231(3)	–0.1658(5)	0.0254(10)
O10	0.3626(1)	–0.0845(1)	0.0861(2)	0.0208(4)	0.3565(3)	–0.0941(3)	0.0875(5)	0.0280(10)
O11	0.2517(1)	–0.1062(1)	–0.1534(2)	0.0226(4)	0.2466(3)	–0.1217(3)	–0.1602(5)	0.0210(9)
O12	0.2227(1)	–0.0206(1)	0.0869(2)	0.0223(4)	0.2180(3)	–0.0302(3)	0.0812(5)	0.0206(9)
O13	0.5762(1)	0.0190(2)	0.0784(2)	0.0233(4)	0.5878(3)	0.0349(3)	0.0648(5)	0.0195(8)
O14	0.6914(1)	0.1107(1)	–0.1570(2)	0.0207(4)	0.6962(3)	0.1165(3)	–0.1828(5)	0.0195(9)
O15	0.7782(1)	0.0775(1)	0.0751(2)	0.0195(4)	0.7944(3)	0.0933(3)	0.0617(6)	0.0248(10)
O16	0.7547(1)	–0.0277(1)	–0.1709(2)	0.0218(4)	0.7633(4)	–0.0207(4)	–0.1787(5)	0.0291(11)
O17	0.6328(1)	–0.1266(1)	0.0706(2)	0.0231(4)	0.6451(3)	–0.1129(3)	0.0692(5)	0.0219(9)
O18	0.5524(2)	–0.0982(2)	–0.1673(2)	0.0281(5)	0.5535(3)	–0.0855(3)	–0.1688(5)	0.0180(8)
	Brandholzite layer at z ≈ ½				**$Co(H_2O)_6[Sb(OH)_6]_2$ layer at *z* ≈ ½**			
Sb4	0	0	0.49757(3)	0.0103(1)	0	0	0.49620(8)	0.0104(1)
Sb5	2/3	1/3	0.42305(4)	0.0101(1)	2/3	1/3	0.48833(7)	0.0119(1)
Sb6	1/3	2/3	0.50490(4)	0.0100(1)	1/3	2/3	0.41225(8)	0.0106(1)
Sb7	0.32739(1)	–0.00737(1)	0.47077(3)	0.0113(1)	0.33208(3)	0.00551(3)	0.46350(5)	0.0125(1)
Sb8	0.66781(1)	0.00662(1)	0.45371(3)	0.0108(1)	0.66045(3)	–0.00523(3)	0.44466(5)	0.0100(1)
O19	0.0648(1)	0.1141(1)	0.3770(2)	0.0157(4)	0.0617(2)	0.1145(2)	0.3751(4)	0.0147(7)
O20	0.1135(1)	0.0411(1)	0.6127(2)	0.0166(4)	0.1146(3)	0.0457(3)	0.6099(4)	0.0172(8)
O21	0.5522(1)	0.2693(1)	0.5424(2)	0.0154(3)	0.7810(3)	0.3748(3)	0.6027(4)	0.0175(8)
O22	0.6218(1)	0.2189(1)	0.3076(2)	0.0173(4)	0.7155(3)	0.2681(3)	0.3667(4)	0.0160(7)
O23	0.2648(1)	0.5522(1)	0.6189(2)	0.0174(4)	0.2184(3)	0.6033(3)	0.5322(5)	0.0163(8)
O24	0.3946(1)	0.7809(1)	0.3844(2)	0.0160(4)	0.4479(3)	0.7357(3)	0.2973(4)	0.0175(8)
O25	0.2607(1)	0.0407(1)	0.3524(2)	0.0193(4)	0.2631(3)	0.0532(3)	0.3474(5)	0.0165(8)
O26	0.3740(1)	0.1100(1)	0.5807(2)	0.0166(3)	0.3816(3)	0.1210(3)	0.5767(5)	0.0166(8)
O27	0.4435(1)	0.0564(1)	0.3556(2)	0.0163(3)	0.4469(3)	0.0718(3)	0.3425(5)	0.0176(8)
O28	0.3965(1)	–0.0510(1)	0.5901(2)	0.0182(4)	0.4038(3)	–0.0409(3)	0.5705(4)	0.0171(8)
O29	0.2803(1)	–0.1236(1)	0.3575(2)	0.0183(4)	0.2805(3)	–0.1100(3)	0.3451(5)	0.0162(8)
O30	0.2117(1)	–0.0734(1)	0.5860(2)	0.0173(4)	0.2189(3)	–0.0640(3)	0.5804(5)	0.0174(8)
O31	0.6215(1)	0.0747(1)	0.5732(2)	0.0177(4)	0.6077(3)	0.0577(3)	0.5575(5)	0.0170(8)
O32	0.7343(1)	0.1190(1)	0.3335(2)	0.0164(3)	0.7320(3)	0.1078(3)	0.3270(5)	0.0161(8)
O33	0.7842(1)	0.0595(1)	0.5679(2)	0.0165(4)	0.7746(3)	0.0488(3)	0.5639(4)	0.0181(8)
O34	0.7100(1)	–0.0652(1)	0.3390(2)	0.0169(4)	0.7092(3)	–0.0744(3)	0.3336(4)	0.0162(8)
O35	0.6074(1)	–0.1073(1)	0.5751(2)	0.0167(4)	0.5929(3)	–0.1200(3)	0.5623(5)	0.0180(8)
O36	0.5500(1)	–0.0413(1)	0.3456(2)	0.0153(3)	0.5478(3)	–0.0516(3)	0.3216(5)	0.0168(8)

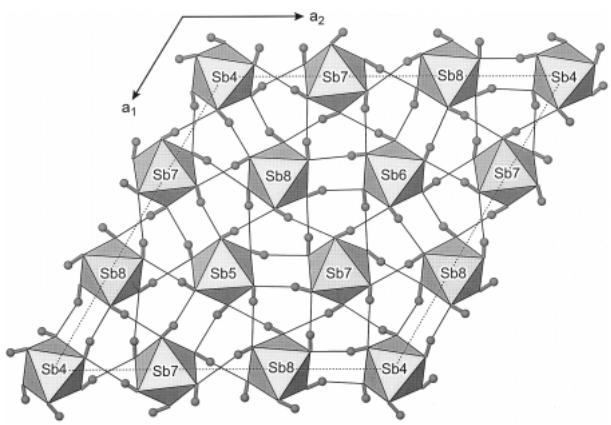

FIGURE 1. Projection of the $\{[Sb(OH)_6]_9\}^{9-}$ layer (at z ≈ 1/2) in brandholzite on (0001). Small circles are H atoms. The unit cell is indicated by the dashed line.

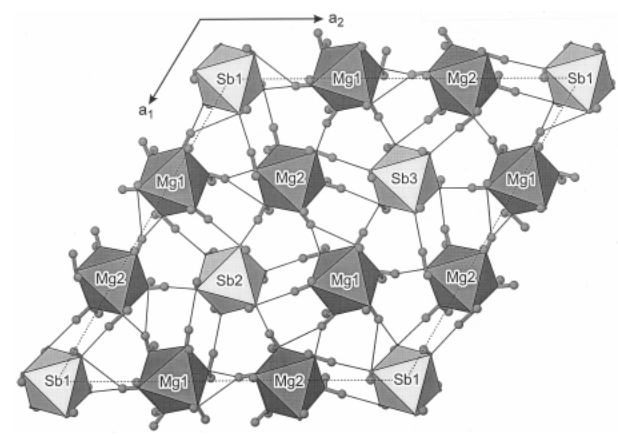

FIGURE 2. Projection of the mixed $\{[Sb(OH)_6]_3[Mg(H_2O)_6]_6\}^{9+}$ layer (at z ≈ 0) in brandholzite on (0001).

TABLE 4. Atomic coordinates of the hydrogen atoms in brandholzite

Atom	*x/a*	*y/b*	*z/c*
H01	0.017(2)	0.099(3)	–0.187(3)
H02	0.101(2)	0.100(2)	0.181(3)
H03	0.573(2)	0.239(2)	–0.263(3)
H04	0.672(2)	0.239(3)	0.085(3)
H05	0.329(2)	0.571(3)	0.196(3)
H06	0.337(2)	0.771(3)	–0.182(3)
H071	0.330(2)	0.150(2)	–0.122(3)
H072	0.339(3)	0.118(2)	–0.222(3)
H081	0.464(2)	0.169(2)	0.074(3)
H082	0.433(3)	0.104(3)	0.178(3)
H091	0.447(2)	0.010(2)	–0.228(3)
H092	0.495(2)	0.090(2)	–0.153(3)
H101	0.349(2)	–0.089(2)	0.169(3)
H102	0.363(2)	–0.126(2)	0.040(3)
H111	0.233(3)	–0.101(2)	–0.250(3)
H112	0.205(2)	–0.146(2)	–0.131(3)
H121	0.178(2)	–0.023(2)	0.051(3)
H122	0.228(3)	–0.003(3)	0.170(3)
H131	0.529(2)	0.012(2)	0.042(3)
H132	0.568(3)	0.009(3)	0.153(3)
H141	0.671(3)	0.106(3)	–0.229(3)
H142	0.687(2)	0.154(2)	–0.114(3)
H151	0.818(2)	0.060(2)	0.089(3)
H152	0.765(3)	0.087(2)	0.156(3)
H161	0.775(3)	0.009(3)	–0.244(3)
H162	0.795(2)	–0.045(2)	–0.155(3)
H171	0.576(2)	–0.162(2)	0.086(3)
H172	0.654(3)	–0.109(3)	0.165(4)
H181	0.500(2)	–0.136(2)	–0.158(4)
H182	0.552(3)	–0.107(3)	–0.250(3)
H19	0.033(2)	0.132(2)	0.372(4)
H20	0.156(2)	0.096(2)	0.599(4)
H21	0.528(2)	0.297(2)	0.555(4)
H22	0.575(2)	0.185(2)	0.328(4)
H23	0.271(2)	0.513(2)	0.607(4)
H24	0.360(2)	0.806(2)	0.375(4)
H25	0.286(2)	0.096(2)	0.356(4)
H26	0.429(2)	0.149(2)	0.558(3)
H27	0.474(2)	0.025(2)	0.349(3)
H28	0.363(2)	–0.110(2)	0.597(4)
H29	0.221(2)	–0.145(2)	0.358(3)
H30	0.189(2)	–0.046(2)	0.595(4)
H31	0.568(2)	0.050(2)	0.573(4)
H32	0.704(2)	0.145(2)	0.308(3)
H33	0.812(2)	0.116(2)	0.572(3)
H34	0.769(2)	–0.042(2)	0.356(4)
H35	0.643(2)	–0.134(2)	0.581(3)
H36	0.514(2)	–0.096(2)	0.366(3)

Notes: U_{iso} =0.037(1)Å^2.

responds well with the sum of the respective ionic radii given by Shannon (1976), 1.98Å. On the other hand, the average Mg-O bond length of 2.057 Å is significantly shorter than expected from crystal chemical considerations. For example, Baur (1981) gives 2.085 Å as average $Mg^{[6]}$-O distance. The bond lengths in synthetic $Mg(H_2O)_6[Sb(OH)_6]_2$ are similar to natural brandholzite with mean values of 1.980 Å for Sb-O and 2.059 Å for Mg-O bonds. Octahedral bond lengths and bond angle variances for brandholzite are in Table 5.

Hydrogen bonding system. For brandholzite, the complex hydrogen bonding scheme of this structure type was established from the refined hydrogen positions. Figure 3 illustrates the arrangement of H-atoms and hydrogen bonds in a projection of the structure on $(10\bar{1}0)$. All hydrogen bonds which are donated by hydroxyl groups of the $\{[Sb(OH)_6]_9\}^{9-}$ unit are located within this layer only. Oxygen donors of hydrogen bonds linking different layers all belong to the mixed $\{[Sb(OH)_6]_3[Mg(H_2O)_6]_6\}^{9+}$ layer. This mixed layer contains enough water molecules to ensure hydrogen bonding within this layer as well as between adjacent layers. Contrary to the situation within the $\{[Sb(OH)_6]_9\}^{9-}$ layers, the OH^- groups of the mixed layers act as donors for further hydrogen bonds among different layers only. Hence, 54 hydrogen atoms per unit cell are involved in hydrogen bonds between adjacent layers and 90 H-atoms are involved in hydrogen bonds within the layers. This general topology is in agreement with the hydrogen bonding scheme proposed by Bonazzi and Mazzi (1996) for bottinoite.

Donor···acceptor distances and D-H···A angles are summarized in Table 6, a complete listing including D-H and H···A distances can be obtained from the authors. Compared to the hydrogen bonding model proposed by Bonazzi and Mazzi (1996), topological differences in brandholzite were found for half of the hydrogen bonds located within the layer at $z \approx 1/2$, which are directed toward acceptors other than the ones proposed for bottinoite.

In general, D···A distances in brandholzite range from 2.699 Å to 3.153 Å. Hydrogen bonds connecting adjacent layers occur between 2.720 Å and 2.953 Å with <D···A> = 2.836 Å, those within the $z \approx 1/2$ layer range from 2.730 Å to 3.153 Å with <D···A> = 2.908Å. Within the z≈ 0 layer, "normal" and bifurcated bonds can be distinguished. The former have D···A from 2.699 Å to 2.749 Å at a mean value of 2.722 Å, the latter scatter from 2.860 Å to 3.132 Å with <D···A> = 3.009 Å. The "normal" hydrogen bonds have O-H···O angles between 154° and 178° with <O-H···O> = 169°, in bifurcated bonds these angles range down to 116° with a mean value of 142°.

Most of the oxygen atoms in brandholzite are fourfold coordinated in strongly distorted tetrahedral arrangements. These oxygen atoms either act as a donor for one and as an acceptor for two hydrogen bonds or vice versa. A few oxygen atoms (O5,7,8,11,12,13,18) are threefold coordinated in more or less pyramidal to planar arrangements. Beside O5, these are water molecules without accepting function in the hydrogen bonding scheme; O5 is a hydroxy group acting as acceptor for only one hydrogen bond.

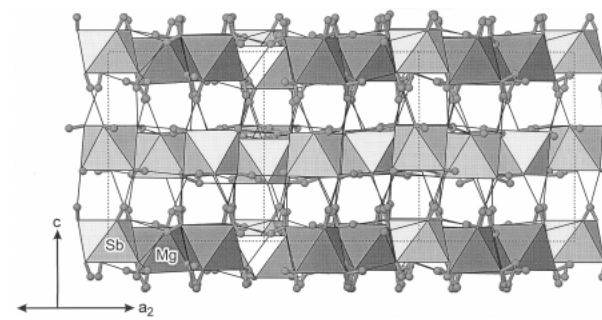

FIGURE 3. Projection of the crystal structure of brandholzite on $(10\bar{1}0)$, showing the hydrogen bonding system and the stacking of layers along [0001]. Sb octahedra are lighter than the Mg octahedra.

TABLE 5. Octahedral bond lengths (Å) and bond angle variances σ^2_{oct} [= (1 / 11)Σ(a_i – 90°)²] in brandholzite (M = Mg) and in $Co(H_2O)_6[Sb(OH)_6]_2$ (M = Co)

	Layer at $z \approx 0$			Layer at $z \approx ½$	
	Brandholzite	M = Co		Brandholzite	M = Co
Sb1–O1 (3×)	1.972(2)	1.979(4)	Sb4–O19 (3×)	1.992(2)	1.994(4)
Sb1–O2 (3×)	1.978(2)	1.966(4)	Sb4–O20 (3×)	1.966(2)	1.961(4)
<Sb1-O>	1.975	1.973	<Sb4–O>	1.979	1.978
σ^2_{oct}	5.03	3.22	σ^2_{oct}	5.44	4.79
Sb2–O3 (3×)	1.976(2)	1.973(4)	Sb5–O21 (3×)	1.988(2)	1.969(4)
Sb2–O4 (3×)	1.972(2)	1.970(4)	Sb5–O22 (3×)	1.972(2)	1.996(4)
<Sb2-O>	1.974	1.972	<Sb5–O>	1.980	1.983
σ^2_{oct}	5.01	4.24	σ^2_{oct}	2.73	5.28
Sb3–O5 (3×)	1.968(2)	1.974(4)	Sb6–O23 (3×)	1.962(2)	1.994(4)
Sb3–O6 (3×)	1.977(2)	1.977(4)	Sb6–O24 (3×)	1.990(2)	1.967(4)
<Sb3-O>	1.973	1.976	<Sb6–O>	1.976	1.981
σ^2_{oct}	4.50	2.27	σ^2_{oct}	4.54	3.01
M1–O7	2.055(2)	2.109(5)	Sb7–O25	1.989(2)	1.997(4)
M1–O8	2.039(3)	2.055(5)	Sb7–O26	1.974(2)	1.964(4)
M1–O9	2.061(2)	2.112(5)	Sb7–O27	1.982(2)	2.001(4)
M1–O10	2.083(2)	2.033(5)	Sb7–O28	1.976(2)	1.967(4)
M1–O11	2.063(2)	2.114(4)	Sb7–O29	1.978(2)	1.992(4)
M1–O12	2.041(2)	2.098(4)	Sb7–O30	1.980(2)	1.965(4)
<M1-O>	2.057	2.087	<Sb7–O>	1.980	1.981
σ^2_{oct}	4.35	5.36	σ^2_{oct}	0.89	1.51
M2–O13	2.061(2)	2.056(5)	Sb8–O31	1.993(2)	1.961(4)
M2–O14	2.064(2)	2.112(5)	Sb8–O32	1.974(2)	1.972(4)
M2–O15	2.051(2)	2.067(5)	Sb8–O33	1.979(2)	1.980(4)
M2–O16	2.071(2)	2.077(5)	Sb8–O34	1.967(2)	1.982(4)
M2–O17	2.053(2)	2.067(5)	Sb8–O35	1.992(2)	1.982(4)
M2–O18	2.035(3)	2.095(4)	Sb8–O36	1.969(2)	1.991(4)
<M2-O>	2.056	2.079	<Sb8–O>	1.979	1.978
σ^2_{oct}	4.41	5.51	σ^2_{oct}	2.70	2.99

TABLE 6. Donor–acceptor hydrogen bond lengths (Å) and corresponding angles (°) in brandholzite

D	H	A	D···A	D–H···A	D	H	A	D···A	D–H···A	D	H	A	D···A	D–H···A
Hydrogen bonds between adjacent layers					**Hydrogen bonds in the layer z ≈ 0**					**Hydrogen bonds in the layer z ≈ ½**				
O1	H01	O20	2.922(3)	168(2)	O7	H071	O14	2.936(3)	144(3)	O19	H19	O25	2.961(2)	168(3)
O2	H02	O19	2.839(3)	167(3)			O15	3.097(3)	140(3)	O20	H20	O33	2.754(2)	168(2)
O3	H03	O21	2.830(3)	171(3)	O8	H081	O4	2.742(3)	177(2)	O21	H21	O31	2.923(2)	175(4)
O4	H04	O22	2.947(3)	166(3)	O9	H092	O3	2.708(2)	169(3)	O22	H22	O27	2.795(2)	162(3)
O5	H05	O24	2.846(3)	178(4)	O10	H102	O6	2.867(3)	171(3)	O23	H23	O35	2.786(2)	178(3)
O6	H06	O23	2.953(3)	170(2)			O5	3.096(2)	116(3)	O24	H24	O29	2.945(2)	176(3)
O7	H072	O26	2.769(3)	157(3)	O11	H112	O17	3.047(3)	141(3)	O25	H25	O32	3.152(2)	169(3)
O8	H082	O27	2.793(3)	167(3)			O16	3.132(2)	141(5)	O26	H26	O21	2.759(2)	162(3)
O9	H091	O28	2.826(3)	164(2)	O12	H121	O1	2.932(2)	160(3)	O27	H27	O36	2.852(2)	176(3)
O10	H101	O29	2.915(3)	166(3)			O2	2.993(2)	123(3)	O28	H28	O23	2.998(2)	174(2)
O11	H111	O30	2.765(3)	171(3)	O13	H131	O10	2.983(2)	134(3)	O29	H29	O34	3.011(2)	169(3)
O12	H122	O25	2.759(3)	171(2)			O9	3.088(2)	150(3)	O30	H30	O20	2.983(2)	177(4)
O13	H132	O36	2.769(3)	168(3)	O14	H142	O4	2.860(3)	164(3)	O31	H31	O28	3.153(2)	171(3)
O14	H141	O31	2.836(3)	169(3)			O3	3.078(2)	123(3)	O32	H32	O22	2.977(2)	163(3)
O15	H152	O32	2.814(3)	175(3)	O15	H151	O2	2.723(1)	175(3)	O33	H33	O26	2.858(2)	178(2)
O16	H161	O33	2.859(3)	163(3)	O16	H162	O1	2.712(2)	177(3)	O34	H34	O19	2.742(1)	154(3)
O17	H172	O34	2.883(3)	173(3)	O17	H171	O5	2.699(2)	178(2)	O35	H35	O30	2.960(2)	173(3)
O18	H182	O35	2.720(3)	156(2)	O18	H181	O6	2.749(2)	168(3)	O36	H36	O24	2.730(2)	160(2)

Crystal structure of $Co(H_2O)_6[Sb(OH)_6]_2$

The crystal structure of synthetic $Co(H_2O)_6[Sb(OH)_6]_2$ can be described as "pseudo-isotypic" to the structures of natural and synthetic $Mg(H_2O)_6[Sb(OH)_6]_2$ and $Ni(H_2O)_6[Sb(OH)_6]_2$, i.e., isolated $Co(H_2O)_6$ and $Sb(OH)_6$ octahedra are arranged in layers as described above and are interconnected by hydrogen bonds only. The most pronounced difference is a significant rotation around the threefold axis of some $Sb(OH)_6$ located on special positions. As illustrated in Figure 4, the octahedra of Sb2 and Sb3 in the mixed layer, and the corresponding octahedra of Sb5 and Sb6 within the $\{[Sb(OH)_6]_9\}^{9-}$ layer are affected, thus enabling to maintain a hydrogen bonding topology comparable to the "brandholzite-type" structures. The rotations seem to be caused by packing requirements due to the different sizes of the $M^{2+}(H_2O)_6$ octahedra. In spite of the larger volume of the $Co(H_2O)_6$ octahedra compared to those of Mg, this results in slightly smaller unit cell dimensions for $Co(H_2O)_6[Sb(OH)_6]_2$.

Octahedral bond lengths and bond angle variances are included in Table 5. The overall mean Sb-O bond length in the Co-compound, 1.978 Å, equals that of brandholzite and hence

TABLE 7. Cell parameters (Å)and *c*/*a* ratios for brucite-type subcells of brandholzite and synthetic analogues $M(H_2O)_6[Sb(OH)_6]_2$ (M = Mg, Co)

	Brandholzite	M = Mg	M = Co
a'	3.102	3.101	3.099
c'	4.934	4.934	4.925
c'/*a*'	1.591	1.591	1.589

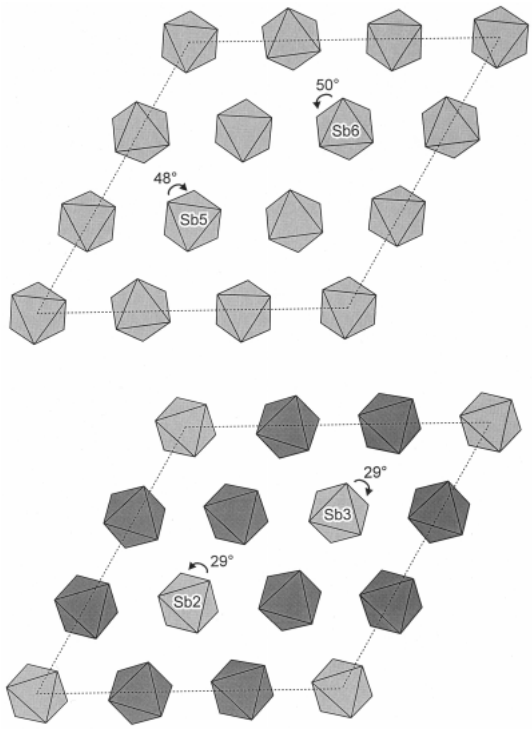

FIGURE 4. Rotation of SbO_6 octahedra in $Co(H_2O)_6[Sb(OH)_6]_2$ (**top:** layer at z ≈ 1/2, **bottom:** layer at z ≈ 0) compared to the positions in brandholzite and synthetic $Mg(H_2O)_6[Sb(OH)_6]_2$. Co bearing octahedra are dark, Sb bearing octahedra light.

complies with crystal chemical expectation discussed above. Similar to the mean Mg-O bond length in brandholzite, the average Co-O distance of 2.083 Å is shorter than the statistically expected value of 2.111 Å (Wildner 1992). On one hand, this might be explained partly by the regular octahedral shape according to the distortion theorem formulated by Brown and Shannon (1973). On the other hand, a coordination by water molecules might result in slightly shortened M-O contacts. This has been shown for Co^{2+}, where the average Co-(H_2O) distance is 2.101 Å (Wildner 1992).

Brucite-type subcells

As discussed in detail by Bonazzi and Mazzi (1996) for bottinoite, the unit cells of brandholzite and $Co(H_2O)_6[Sb(OH)_6]_2$ can accordingly be described as supercells (54 times) of a brucite-type structure. The brucite-type subcells (Table 7) are obtained by applying the transformation matrix [–1/9, –2/9, 0; 2/9, 1/9, 0; 0, 0, 1/2] to the lattice vectors of the antimonates. As found for bottinoite, the resulting *c*/*a* ratios are greater than those of various brucite-like structures, but smaller than the value 1.633 for an ideal hexagonal close packed structure. Following Bonazzi and Mazzi (1996), this is explained by the practically regular shape of the $M^{2+}O_6$ octahedra in the title compounds compared to the rather strongly flattened octahedra in the brucite structure type, combined with an expansion of the *a* axis due to the unfilled positions within the octahedral layers.

ACKNOWLEDGMENTS

The authors thank S. Meier, Marktredwitz, who kindly provided the brandholzite sample. Thanks are also due to Th. Ntaflos, Vienna, for his help with the electron microprobe measurements. Financial support by the International Centre for Diffraction Data, ICDD, Newtown Square, Pennsylvania, 19073-3273, U.S.A. under grant no. ET90-03 is gratefully acknowledged.

REFERENCES CITED

Balitcheva, T.G. and Roi, N.I. (1971) IR spectra and structure of several crystalline hexahydroxyantimonates and their deutero analogs. Journal of Structural Chemistry, 12, 384–390.

Baur, W.H. (1981) Interatomic distance predictions for computer simulation of crystal structures. In M. O'Keefe and A. Navrotsky, Eds., Structure and bonding in crystals, Vol. II, 31–52. Academic Press, New York.

Beintema, J. (1936) On the crystal-structure of magnesium- and nickel antimonate. Proceedings of the Royal Academy of Sciences of Amsterdam, 39, 241–252.

Bonazzi, P. and Mazzi, F. (1996) Bottinoite, $Ni(H_2O)_6[Sb(OH)_6]_2$: Crystal structure, twinning, and hydrogen bond model. American Mineralogist, 81, 1494–1500.

Brown, I.D. and Shannon, R.D. (1973) Empirical bond-strength-bond-length curves for oxides. Acta Crystallographica A, 29, 266–282.

Fischer, R.X. and Tillmanns, E. (1988) The equivalent isotropic displacement factor. Acta Crystallographica C, 44, 775–776.

Franck, R. (1973) Spectres d'absorption infrarouge de quelques hydroxyantimoniates. Revue de chimie minérale, 10, 795–810.

Haushofer, K. (1880) Über die mikroskopischen Formen einiger bei der Analyse vorkommenden Verbindungen. Zeitschrift für Kristallographie, 4, 42–56.

Heffter, L. (1852) Poggendorff's Annalen der Physik und Chemie, 86, 418.

Mandarino, J.A. (1976) The Gladstone-Dale relationship, part I. Derivation of new constants. Canadian Mineralogist, 14, 498–502.

Mandarino, J.A. (1981) The Gladstone-Dale relationship, part IV. The compatibility concept and its application. Canadian Mineralogist, 19, 441–450.

Shannon, R.D. (1976) Revised effective ionic radii and systematic studies of interatomic distances in halides and chalcogenides. Acta Crystallographica A, 32, 751–767.

Stettner, G. (1980) Zum geologischen Aufbau des Fichtelgebirges. Der Aufschluss, 31, 391–403.

Wildner, M. (1992) On the geometry of $Co(II)O_6$ polyhedra in inorganic compounds. Zeitschrift für Kristallographie, 202, 51–70.

MANUSCRIPT RECEIVED MAY 19, 1999
MANUSCRIPT ACCEPTED NOVEMBER 8, 1999
PAPER HANDLED BY BRYAN CHAKOUMAKOS